

# Classification of error-related potentials evoked during observation of human motion sequences<sup>\*</sup>

Su Kyoung Kim<sup>1</sup>[0000–0002–9261–2252], Julian Liersch<sup>2</sup>[0000–0003–0521–3796], and  
Elsa Andrea Kirchner<sup>1,3</sup>[0000–0002–5370–7443]

<sup>1</sup> Robotics Innovation Center,  
German Research Center for Artificial Intelligence (DFKI), Bremen, Germany  
`su-kyoung.kim@dfki.de`

<sup>2</sup> Robotics Lab, Faculty of Mathematics and Computer Science,  
University of Bremen, Germany  
`jliersch@uni-bremen.de`

<sup>3</sup> Institute of Medical Technology Systems, University of Duisburg-Essen, Germany  
`elsa.kirchner@uni-due.de`

**Abstract.** In recent studies, electroencephalogram (EEG)-based interfaces that enable to infer human intentions and to detect implicit human evaluation contributed to the development of effective adaptive human-machine interfaces. In this paper, we propose an approach to allow systems to adapt based on implicit human evaluation which can be extracted by using EEGs. In our study, human motion segments are evaluated according to an EEG-based interface. The goal of the presented study is to recognize incorrect motion segments before the motion sequence is completed. This is relevant for early system adaptation or correction. To this end, we recorded EEG data of 10 subjects while they observed human motion sequences. Error-related potentials (ErrPs) are used to recognize observed erroneous human motion. We trained an EEG classifier (i.e., ErrP decoder) that detects erroneous motion segments as part of motion sequences. We achieved a high classification performance, i.e., a mean balanced accuracy of 91% across all subjects. The results show that it is feasible to distinguish between correct and incorrect human motion sequences based on the current intentions of an observer. Further, it is feasible to detect incorrect motion segments in human motion sequences by using ErrPs (i.e., implicit human evaluations) before a motion sequence is completed. This is possible in real time and especially before human motion sequences are completed. Therefore, our results are relevant for human-robot interaction tasks, e.g., in which model adaptation of motion prediction is necessary before the motion sequence is completed.

**Keywords:** error-related potentials (ErrPs), brain-computer interfaces (BCIs), human motion sequences, human-machine interaction

---

<sup>\*</sup> Supported by the Federal Ministry for Economic Affairs and Climate Action (BMWK) FKZ: 50RA2023 and 50RA2024 and Federal Ministry for Education and Research (BMBF) FKZ: 01IW21002.

## 1 Introduction

Inference of future human behavior and intentions is essential for an effective adaptive human-machine interaction. In particular, electroencephalogram (EEG)-based interfaces, e.g., brain-computer interfaces, enable systems to perform such inference and thus to flexibly adapt to human intentions, expectations, motion planning, or implicit evaluations of behavior [5, 11, 14–16, 18–20]. In recent years, it could be shown that EEG-based interfaces enable continuous adaptive learning of systems (e.g., robots). For example, a robot learns and updates a policy based on human intrinsic evaluation (e.g., EEG-based feedback). The robot chooses a correct action that corresponds to the current context (human gesture) according to the EEG-based feedback, where the current context is unknown to the robot (i.e., the meaning of the human gestures is unknown and may change depending on the current human intention) [16, 18]. Such applications are mostly shown in robot learning, e.g., adaptation of learning algorithms. Therefore, EEG-based interfaces are a good choice for human-in-the-loop approaches such as human-robot interaction, especially when continuous access to human intrinsic feedback is required.

Human intention can be inferred in various ways, e.g., by analyzing human motion sequences, human gestures, human EEGs as well as other biosignals such as electromyogram (EMG), etc. That means, human intention can be inferred by accessing both explicit (e.g., human motion, gesture) and implicit data (e.g., ErrP in the EEG). We propose an approach to allow systems (e.g., robots) to adapt based on human intention. In our application, we extracted human intentions by analyzing human motion and inferring implicit human evaluations by EEG analysis. For motion analysis, we trained a motion analyzer that segments trajectories, classifies segmented trajectories, and predicts the next motion segments in motion sequences (Fig. 1, blue boxes and lines). For EEG analysis, we trained an EEG classifier to detect/recognize erroneous motions segments while observing human motion sequences. Specifically, we used EEG to detect motion segments (as part of motion sequences) that have been defined as “incorrect” in the current situation (context). To enable this detection, we used error-related potentials (ErrPs), which are elicited in the human brain, for example, when observing erroneous behavior. In this paper, we focus on EEG analysis.

The ErrP is a well established event-related potential (ERP) component, which has been applied in several research and application areas (see, review, [5]). Like other ERP components (P300, MRCP, etc., details, see [13]), ErrPs have been applied in brain-computer interfaces (BCIs), human-machine interactions (HMIs), and human-robot interactions (HRIs). In many cases, ErrPs have been investigated in observation tasks, e.g., observations of motions of an abstract entity [12, 14, 24, 26] or observations of motion of robots on a monitor [9, 23], or observations of motion of real robots [8, 10, 16, 17, 23, 29]. Further, ErrPs have been used not only to correct erroneous actions of the robot [29], but also to learn or adjust the behavioral strategy of robots [11, 16, 18]. In recent studies, ErrPs have been applied in HRIs, i.e., a robot learns a behavior strategy through interactions with humans. Here, the robot learns a behavior strategy not only

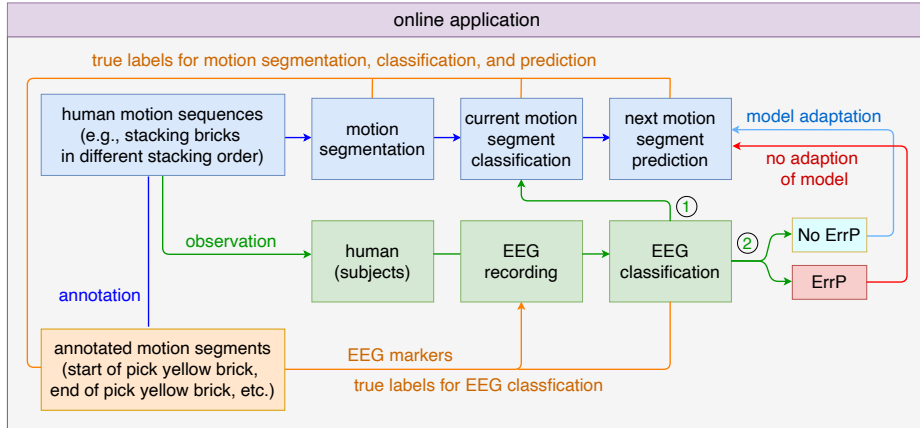


Fig. 1. Concept of our approach

by updating the strategy based on implicit human evaluation (i.e., the correctness of robot’s behavior) via BCIs, but also by interpreting human intentions e.g., from human gestures [16, 18]. To our knowledge, there are no publications that investigate the use of ErrPs when observing *real human movements* or *real human motion sequences*. However, there is one study in which ErrPs were elicited when observing simulated human hand movements [27]. In [27], subjects’ grasping movements were simulated in a virtual reality (VR) environment, and subjects observed their own hand movements simulated in a VR environment in which hand movements were simplified.

In our approach, EEG analysis can be applied in two ways (Fig. 1, green boxes and lines). First, EEG classifications (e.g., the presence of ErrP) can be used to correct erroneous results of the motion analyzer (e.g., misclassification of motion segments). Second, EEG classification can be used to control a potential model adaptation (e.g., retraining) of the motion analyzer. That means, we can use EEG analysis both for direct correction of erroneous outputs of the motion analyzer as well as for model adaptation of the motion analyzer.

As mentioned above, in this paper, we focus on EEG analysis and evaluation of EEG classifiers. For training an EEG classifier, a reasonable amount of training instances is required to avoid overfitting. Thus, we recorded videos of human motion sequences to be used as EEG stimuli in various context, i.e., various stacking orders in our scenario (Fig. 2). In our scenario, a motion sequence of the stacking process consists of eight motion segments, which can be arranged into different sequences depending on human intention (Fig. 2). The goal of our study is to detect erroneous motion segments before the motion sequences are completed in order to adjust the systems according to the EEG classification even before the motion is completed. To this end, we recorded EEGs while observing human motion sequences and trained subject-specific EEG classifiers (i.e., ErrP

decoders) that detect erroneous motion segments as part of motion sequences, i.e., before the entire motion sequence is completed.

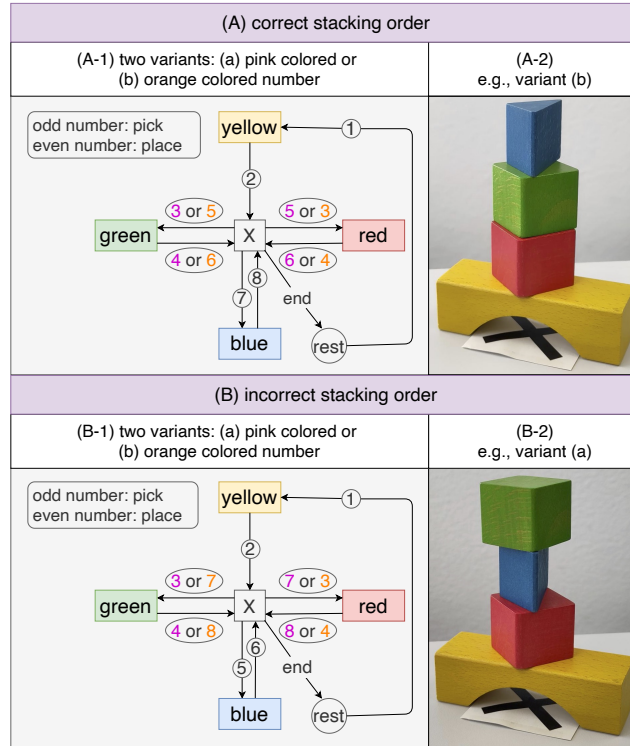


**Fig. 2.** Concept of motion sequences for correct and incorrect stacking orders (A, B). We have two variants each to stack in correct and incorrect order (A-1, B-1). For each condition, an example of the correct and incorrect stacking order is shown (A-2, B-2).

## 2 Methods

**Experimental setup** We designed an experiment, in which ten subjects observed video recordings of human motions on a monitor. To this end, we recorded videos, in which a person stacks four colored bricks (yellow, green, red, and blue) in different orders (see Fig. 2). The motion sequences of the stacking process consist of eight motion segments (“pick yellow”, “place yellow”, “pick red”, “place red”, “pick green”, “place green”, “pick blue”, and “place blue”), which can be arranged into different sequences (Fig. 3) depending on human intention.

We defined two conditions for training an EEG classifier (Fig. 2 A, B). First, we defined the stacking order as correct, if the blue brick was on top and the

yellow brick was at the bottom of the resulting stack (e.g., Fig. 2A-2). This results in two correct stacking variants (Fig. 2A-1). Second, if the blue brick was placed as the third brick instead of on the top (e.g., Fig. 2B-2), we defined the stacking order as incorrect. This resulted in two incorrect stacking variants (Fig. 2B-1).

We annotated the motion segments (e.g., “pick blue” for reaching for and picking up the blue brick) in the videos. Based on the annotation, markers at the start of the motion segments were sent to the EEG recording, when the corresponding video frame was displayed on the monitor. These markers were labeled based on the position of the corresponding motion segments in the stacking orders (Fig. 2A-1, Fig. 2B-1). For example for the start of the segment “pick blue” in the correct condition the marker S7 is used (Fig. 3A). We defined these markers as EEG markers, which were used to segment the EEG data stream into epochs for training a classifier (Fig. 4). In this paper, only the markers S5 in the incorrect condition and S6 and S7 in the correct condition are used (Fig. 3).

**Data recording** Ten subjects participated in the experiment. We recorded EEG data while the subjects observed the videos of human motion sequences. EEGs were recorded at 500 Hz with a 64-channel amplifier (LiveAmp, Brain Products GmbH) using an extended 10-20 electrode system with the reference electrode at FCz (actiCapSlim, Brain Products GmbH). EEG markers were sent to the EEG data stream in real time (Fig. 4).

Ten datasets were recorded in a single session for each subject. Each dataset contained the EEG data for observing 25 videos, i.e., 20 videos with correct stacking order and 5 videos with incorrect stacking order. That means, the class ratio was 1:4 with respect to incorrect and correct stacking order. Due to the class imbalance a stratified cross validation was used for evaluation and the classes were differently weighted for classifier training (details, see section 2. Evaluation and section 2. EEG processing respectively).

**EEG processing** The EEG processing pipeline consists of three steps: pre-processing, feature extraction and classification. For EEG processing, we used pySPACE [21], in which relevant methods are implemented (e.g., xDAWN [28]) or external packages (e.g., libSVM [4], pyriemman [1]) are integrated.

The EEG data stream was segmented into epochs from 0s to 1s and labeled as “correct” or “incorrect” based on EEG markers (section 2. Experimental setup and Fig. 3). All epochs were band pass filtered using Fast Fourier Transform (FFT) with a pass band from 0.1 to 12 Hz<sup>4</sup>, decimated to 50 Hz, and normalized to have zero mean for each channel.

For feature extraction, we combined xDAWN and a Riemmanian manifold approach [6,30]. Using xDAWN, we reduced the 64 physical channels to 5 pseudo channels, in which the signal-to-noise ratio for the “incorrect” class is maximized. All epochs were projected into the pseudo channels that consist of 50

<sup>4</sup> Potential artifacts due to the Gibbs phenomenon can be neglected here, as only the classification of the signals and not their shape is of interest.

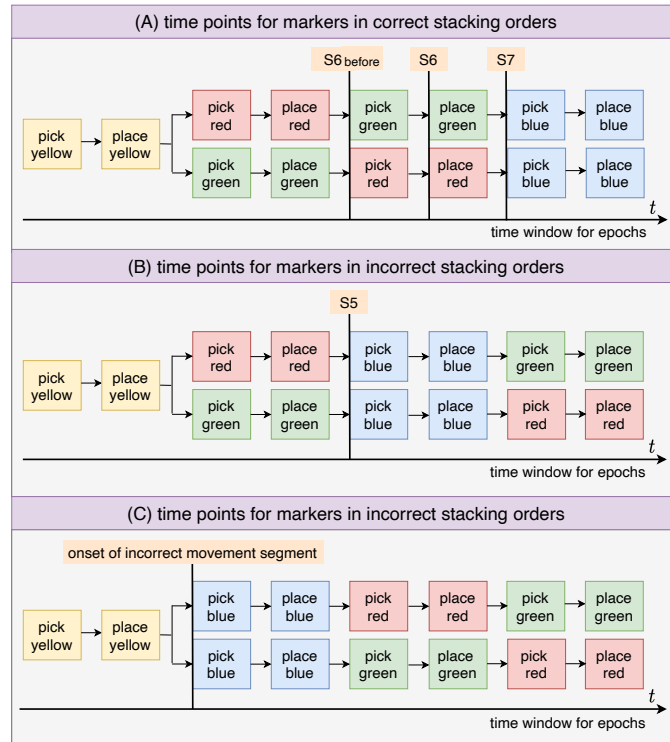


**Fig. 3.** Concepts of EEG markers in both correct and incorrect condition (A, B). The time points at which markers are sent to the EEG recordings are visualized with vertical lines with the names for the corresponding markers above. The subfigures A and B are analogous to Fig. 2. The time point used for classifier transfer (details, see section 4. Discussion) is depicted in C. EEGs are segmented according to EEG markers (details, see section 2. EEG processing).

data points, i.e., we obtained 250 data points ( $5 \text{ channels} \times 50 \text{ data points}$ ) after applying xDAWN. After applying xDAWN, we used a Riemannian manifold approach [6,30]. To this end, we generated *extended epochs* (cf. [2]) so that we obtained 10 pseudo channels ( $5 \cdot 2 = 10 \text{ channels}$ ). A  $10 \times 10$ -dimensional covariance matrix was estimated across the 50 data points for each of the extended epochs using the shrinkage regularized estimator of Ledoit-Wolf [22], which ensures that the estimated covariance matrices are positively defined. After the estimation of the covariance matrices, we approximated their Riemannian center of mass<sup>5</sup> [3], which is used as reference point to append a tangent space. All training and testing data (i.e., each epoch) were projected into this tangent space and vectorized using Mandel notation [25]. Using Mandel notation, we reduced the symmetric

<sup>5</sup> The Riemannian center of mass is also called geometric mean in the field of BCI or Fréchet mean in general.

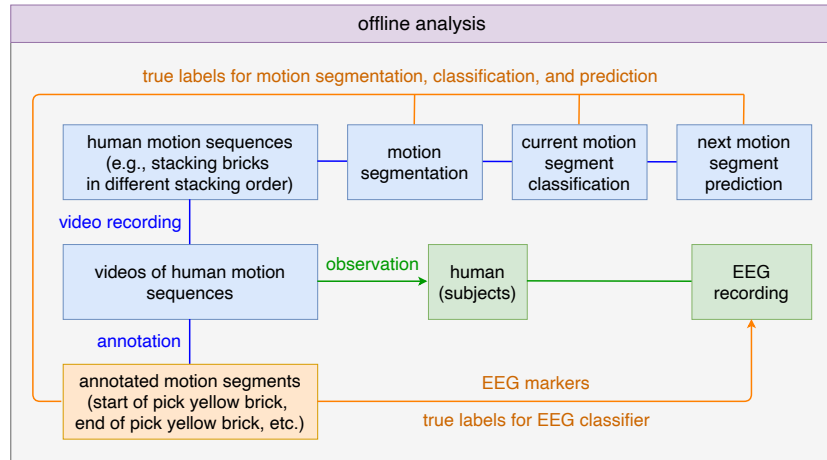


**Fig. 4.** Experimental setup for EEG recording. The concept the offline analysis performed in the study is illustrated.

$10 \times 10$ -dimensional matrices into 55-dimensional feature vectors. In the end, we Z-score normalized the feature vectors.

For classification, we used a linear Support Vector Machine (SVM) [7]. The hyperparameter  $C$  of the SVM was selected from  $\{10^{-6}, 10^{-5}, 10^{-4}, 10^{-3}, 10^{-2}, 10^{-1}, 1\}$  using a five-fold stratified cross validation on the current training data and the classes were weighted as 2:1  $\sim$  “incorrect” : “correct” in the formulation of the optimization problem.

**Evaluation** For evaluation, we used three EEG markers (i.e., three labels, see Fig. 3). The evaluations were performed for each of the ten subjects individually. Either S6 or S7 was used as the marker for the correct class (Fig. 3A). In both cases, S5 was used for the incorrect class (Fig. 3B). As mentioned in section 2. Data recording, we recorded 10 datasets for each subject. First, we concatenated the epochs of the 10 datasets, resulting in 200 correct and 50 incorrect epochs. A  $5 \times 5$  stratified cross validation was applied on the concatenated datasets. By averaging across the folds and repetitions, we obtained classification performances for each of the 10 subjects. For performance metric, we used a balanced accuracy, i.e., the arithmetic mean of true positive rate (TRP) and true negative rate (TNR). Note that the positive class stands for incorrect stacking order and negative class stands for correct stacking order.

### 3 Results

Table 1 shows the classification performance for each subject in both label combinations (label S6 vs. label S5; label S7 vs. label S5). In addition, we reported the means and standard errors as well as the medians across all subjects. In

average, we achieved 91% and 79% for label S6 vs. label S5 and label S7 vs. label S5 respectively. However, one subject (subject 9) was found to have lower performance compared to the other subjects. This subject reported after the experiment that he had difficulty concentrating on watching the videos. Further, the use of S6 yielded a better classification performance than the use of S7 for the correct class. This result pattern, i.e., the superior performance by using S6 compared to the use of S7, was observed for all subjects.

**Table 1.** EEG classification performance: mean balanced accuracies ( $\text{bACC}=(\text{TPR}+\text{TNR})/2$ ) of  $5 \times 5$  stratified cross validation for each subject. Two labels (label S6 and label S7) for correct class were used for comparison. For incorrect class, only one label (label S5) was used for evaluation. The mean and standard error of the mean (SEM) are given. In addition, the median is reported.

subject	label S6 vs. label S5			label S7 vs. label S5		
	TPR (%)	TNR (%)	bACC (%)	TPR (%)	TNR (%)	bACC (%)
1	96.0	99.5	97.8	76.8	89.8	83.3
2	82.0	94.8	88.4	62.8	89.6	76.2
3	84.4	97.1	90.8	74.4	90.3	82.4
4	81.2	96.2	88.7	69.2	89.0	79.1
5	89.6	94.5	92.1	71.6	91.1	81.4
6	97.2	99.5	98.4	74.0	89.8	81.9
7	90.4	97.3	93.9	79.6	96.6	88.1
8	90.4	97.2	93.8	68.4	90.3	79.4
9	55.6	89.6	72.6	42.4	84.6	63.5
10	86.0	97.7	91.9	68.4	89.9	79.2
mean $\pm$ SEM	85.3 $\pm$ 3.7	96.3 $\pm$ 0.9	90.8 $\pm$ 2.3	68.8 $\pm$ 3.3	90.1 $\pm$ 0.9	79.4 $\pm$ 2.0
median	87.8	97.2	92.0	70.4	89.9	80.4

## 4 Discussion

In this paper, we evaluated EEG data segmented based on the labels S6 and S7 for the correct class (Fig. 2A-1, Fig. 3A) and the label S5 for the incorrect class (Fig. 2B-1, Fig. 3B). The classification performance was higher when using the label S6 than when using the label S7 for the correct class (Table 1). This indicates that, as expected, subjects already recognized the correct stacking orders when they observed the placement of the red or green brick as the third brick (Fig. 2B-1, Fig. 3B), i.e., before the blue brick was picked (label S7). If our assumption is correct, the use of the label  $S6_{\text{before}}$  for the correct class (Fig. 3B) could also improve the classification performance compared to use of the label S7. This should be investigated in the future work. Further, the decreased classification performance when using label S7 compared to label S6 may be caused

by subjects paying less attention to the videos after S6. This reduced attention might have resulted in less relevant features for distinction between the correct and incorrect class.

In this study, we used only the videos showing that the blue brick was placed as the third brick for the incorrect stacking order (Fig. 2B-1, B-2). That means, the stacking orders are different between two variants of incorrect condition, but the position of the blue bricks (incorrect motion segments) in the stacking order was the same (Fig. 3B). However, it should in principle be feasible to detect ErrPs in any other position in the stacking sequence as well (e.g., Fig. 3B vs. C). Thus, we tested our approach in case of context change, i.e., the position of incorrect motion segments as part of motion sequences is changed. That means, we also detected incorrect motion segments, in which the blue brick is placed as the second brick for the incorrect condition (Fig. 3C). Here, we achieved a bACC of 98.4%. This classification performance was comparable with the case of Fig. 3B (Fig. 3B vs. Fig. 3C: 98.4% vs. 97.8% for label S6 vs. label S5). Further, we tested a classifier transfer approach on one subject, i.e., the classifier trained on incorrect motion segments in Fig. 3B was applied to the test data containing incorrect motion segments in Fig. 3C. Our preliminary results suggest that it is even feasible to transfer an ErrP classifier trained to detect an incorrect placement of the blue brick as the third (Fig. 3B) to detect motion segments, in which the blue brick was placed as the second brick for the incorrect condition (Fig. 3B). Here, we obtained a bACC of 88.7%. In a preliminary study, we evaluated the classifier transfer on one subject (Subject 1). Future work should systematically investigate the classifier transfer approach with an appropriate sample size.

For sending markers at the start of the motion segments, we used manual annotations of the motion segments in the observed videos. This is infeasible in real-time applications of ErrP detection when observing human motion. Instead, the time points of the start of the motion segments could be estimated by an online motion analysis. Thus, in future work, we will send markers directly from the motion analyzer online to the EEG recordings instead of from video annotations.

Our results show that it is feasible to distinguish between correct and incorrect human motion sequences based on the current intentions of an observer. This is possible in real time and especially before human motion sequences are completed. Therefore, our results are relevant to human-robot interaction tasks, since robots can adapt their behavioral strategy or interaction strategy „on the fly”. On the one hand, we can use our approach described in Fig. 1, in which a motion classifier or a motion predictor can be adapted or not according to ErrP-based human evaluations. On the other hand, our approach can be applied to adapt robot behavior. If we detect ErrP-based evaluations of erroneous robot motion segments before the robot motion trajectories are completed, we can directly adjust the model underlying the control of the robot trajectories.

## References

1. Barachant, A., Barthélemy, Q., King, J.R., Gramfort, A., Chevallier, S., Rodrigues, P.L.C., Olivetti, E., Goncharenko, V., vom Berg, G.W., Reguig, G., Lebeurrier, A., Bjäreholt, E., Yamamoto, M.S., Clisson, P., Corsi, M.C.: pyriemann/pyriemann: v0.3 (Jul 2022). <https://doi.org/10.5281/zenodo.7547583>
2. Barachant, A., Congedo, M.: A Plug&Play P300 BCI Using Information Geometry. <https://doi.org/10.48550/arXiv.1409.0107>
3. Cartan, E.J.: Groupes simples clos et ouverts et géométrie riemannienne. *Journal de Mathématiques Pures et Appliquées* **8**, 1–34 (1929)
4. Chang, C.C., Lin, C.J.: LIBSVM: A library for support vector machines. *ACM Transactions on Intelligent Systems and Technology (TIST)* **2**(3), 27:1–27 (May 2011). <https://doi.org/https://doi.org/10.1145/1961189.1961199>
5. Chavarriaga, R., Sobolewski, A., Millán, J.D.R.: Errare machinale est: The use of error-related potentials in brain-machine interfaces. *Frontiers in Neuroscience* **8**, 208 (2014). <https://doi.org/10.3389/fnins.2014.00208>
6. Congedo, M., Barachant, A., Bhatia, R.: Riemannian geometry for EEG-based brain-computer interfaces; a primer and a review. *Brain-Computer Interfaces* **4**(3), 155–174 (2017). <https://doi.org/10.1080/2326263X.2017.1297192>
7. Cortes, C., Vapnik, V.: Support-vector networks. *Machine Learning* **20**(3), 273–297 (1995). <https://doi.org/10.1007/BF00994018>
8. Ehrlich, S., Cheng, G.: A neuro-based method for detecting context-dependent erroneous robot action. In: 2016 IEEE-RAS 16th International Conference on Humanoid Robots (Humanoids). pp. 477–482 (2016). <https://doi.org/10.1109/HUMANOIDS.2016.7803318>
9. Iturrate, I., Montesano, L., Minguez, J.: Robot reinforcement learning using eeg-based reward signals. In: 2010 IEEE international conference on robotics and automation. pp. 4822–4829. IEEE (2010). <https://doi.org/10.1109/ROBOT.2010.5509734>
10. Iturrate, I., Montesano, L., Minguez, J.: Single trial recognition of error-related potentials during observation of robot operation. In: 2010 Annual International Conference of the IEEE Engineering in Medicine and Biology. pp. 4181–4184. IEEE (2010). <https://doi.org/10.1109/IEMBS.2010.5627380>
11. Iturrate, I., Chavarriaga, R., Montesano, L., Minguez, J., Millán, J.d.R.: Teaching brain-machine interfaces as an alternative paradigm to neuroprosthetics control. *Scientific Reports* **5**, 13893 (2015). <https://doi.org/10.1038/srep13893>
12. Iturrate, I., Grizou, J., Omedes, J., Oudeyer, P.Y., Lopes, M., Montesano, L.: Exploiting Task Constraints for Self-Calibrated Brain-Machine Interface Control Using Error-Related Potentials. *PLoS ONE* **10**(7), e0131491 (2015). <https://doi.org/10.1371/journal.pone.0131491>
13. Kappenman, E.S., Luck, S.J.: *The Oxford Handbook of Event-Related Potential Components*. Oxford University Press (12 2011). <https://doi.org/10.1093/oxfordhb/9780195374148.001.0001>
14. Kim, S.K., Kirchner, E.A.: Classifier Transferability in the Detection of Error Related Potentials from Observation to Interaction. In: 2013 IEEE International Conference on Systems, Man, and Cybernetics. pp. 3360–3365 (2013). <https://doi.org/10.1109/SMC.2013.573>
15. Kim, S.K., Kirchner, E.A.: Handling few training data: classifier transfer between different types of error-related potentials. *IEEE Transactions on Neural Systems and Rehabilitation Engineering* **24**(3), 320–332 (2016). <https://doi.org/10.1109/TNSRE.2015.2507868>

16. Kim, S.K., Kirchner, E.A., Kirchner, F.: Flexible online adaptation of learning strategy using EEG-based reinforcement signals in real-world robotic applications. In: 2020 IEEE International Conference on Robotics and Automation (ICRA). pp. 4885–4891 (2020). <https://doi.org/10.1109/ICRA40945.2020.9197538>
17. Kim, S.K., Kirchner, E.A., Schloßmüller, L., Kirchner, F.: Errors in Human-Robot Interactions and Their Effects on Robot Learning. *Frontiers in Robotics and AI* **7** (2020). <https://doi.org/10.3389/frobt.2020.558531>
18. Kim, S.K., Kirchner, E.A., Stefes, A., Kirchner, F.: Intrinsic interactive reinforcement learning – Using error-related potentials for real world human-robot interaction. *Scientific Reports* **7** (2017). <https://doi.org/10.1038/s41598-017-17682-7>
19. Kirchner, E.A., Fairclough, S.H., Kirchner, F.: Embedded multimodal interfaces in robotics: Applications, future trends, and societal implications. In: Monash University, Oviatt, S., Schuller, B., University of Augsburg and Imperial College London, Cohen, P.R., Monash University, Sonntag, D., German Research Center for Artificial Intelligence (DFKI), Potamianos, G., University of Thessaly, Krüger, A., Saarland University and German Research Center for Artificial Intelligence (DFKI) (eds.) *The Handbook of Multimodal-Multisensor Interfaces: Language Processing, Software, Commercialization, and Emerging Directions - Volume 3*. Association for Computing Machinery (2019). <https://doi.org/10.1145/3233795.3233810>
20. Kirchner, E.A., Kim, S.K., Straube, S., Seeland, A., Wöhrle, H., Krell, M.M., Tabie, M., Fahle, M.: On the Applicability of Brain Reading for Predictive Human-Machine Interfaces in Robotics. *PLOS ONE* **8**(12), e81732 (2013). <https://doi.org/10.1371/journal.pone.0081732>
21. Krell, M., Straube, S., Seeland, A., Wöhrle, H., Teiwes, J., Metzen, J., Kirchner, E., Kirchner, F.: pySPACE—a signal processing and classification environment in Python. *Frontiers in Neuroinformatics* **7** (2013). <https://doi.org/10.3389/fninf.2013.00040>
22. Ledoit, O., Wolf, M.: A well-conditioned estimator for large-dimensional covariance matrices. *Journal of Multivariate Analysis* **88**(2), 365–411 (2004). [https://doi.org/10.1016/S0047-259X\(03\)00096-4](https://doi.org/10.1016/S0047-259X(03)00096-4)
23. Lopes-Dias, C., Sburlea, A.I., Breitegger, K., Wyss, D., Drescher, H., Wildburger, R., Müller-Putz, G.R.: Online asynchronous detection of error-related potentials in participants with a spinal cord injury using a generic classifier. *Journal of Neural Engineering* **18**(4), 046022 (2021). <https://doi.org/10.1088/1741-2552/abd1eb>
24. Lopes-Dias, C., Sburlea, A.I., Müller-Putz, G.: Masked and unmasked error-related potentials during continuous control and feedback. *Journal of Neural Engineering* **15** (2018). <https://doi.org/10.1088/1741-2552/aab806>
25. Mandel, J.: Generalisation de la theorie de plasticite de W. T. Koiter. *International Journal of Solids and Structures* **1**(3), 273–295 (1965). [https://doi.org/10.1016/0020-7683\(65\)90034-X](https://doi.org/10.1016/0020-7683(65)90034-X)
26. Omedes, J., Iturrate, I., Minguez, J., Montesano, L.: Analysis and asynchronous detection of gradually unfolding errors during monitoring tasks. *Journal of neural engineering* **12**, 056001 (2015). <https://doi.org/10.1088/1741-2560/12/5/056001>
27. Pavone, E.F., Tieri, G., Rizza, G., Tidoni, E., Grisoni, L., Aglioti, S.M.: Embodying others in immersive virtual reality: electro-cortical signatures of monitoring the errors in the actions of an avatar seen from a first-person perspective. *Journal of Neuroscience* **36**(2), 268–279 (2016). <https://doi.org/10.1523/JNEUROSCI.0494-15.2016>
28. Rivet, B., Souloumiac, A., Attina, V., Gibert, G.: xDAWN Algorithm to Enhance Evoked Potentials: Application to Brain–Computer Interface.

- IEEE Transactions on Biomedical Engineering **56**(8), 2035–2043 (2009). <https://doi.org/10.1109/TBME.2009.2012869>
29. Salazar-Gomez, A.F., DelPreto, J., Gil, S., Guenther, F.H., Rus, D.: Correcting robot mistakes in real time using EEG signals. In: 2017 IEEE International Conference on Robotics and Automation (ICRA). pp. 6570–6577 (2017). <https://doi.org/10.1109/ICRA.2017.7989777>
  30. Yger, F., Berar, M., Lotte, F.: Riemannian Approaches in Brain-Computer Interfaces: A Review. IEEE Transactions on Neural Systems and Rehabilitation Engineering **25**(10), 1753–1762 (2017). <https://doi.org/10.1109/TNSRE.2016.2627016>